UTILIZATION OF CERAMIC FILTERS TO PRODUCE CLEANER SUPERALLOY MELTS

D. Apelian* and W.H. Sutton†

*Professor and Head, Department of Materials Engineering,
Drexel University, Philadelphia, PA 19104, USA

†Associate Director of Technology, Special Metals Corporation,
New Hartford, NY 13413, USA

Introduction

The need for cleanliness and tighter control over the content and size of nonmetallic particulates (inclusions) in superalloys is a real and severe one. The newer, advanced superalloys for jet engines are continually being subjected to significantly higher stresses and service temperatures than their earlier predecessors. As a result, the tolerance levels for defects in these alloys has markedly decreased in recent years. Defects ranging from 0.05 - 0.76 mm (0.002-0.03 inches) can be of critical size in highly alloyed superalloys operating under highly stressed LCF conditions. Such defects are one to two orders of magnitude smaller than those tolerated by the conventionally processed wrought alloys (1).

Defects in superalloys may manifest themselves as microporosity, intermetallic segregates, nitride and carbide stringers, and other nonmetallic inclusions (2-4). The first two types of defects can be controlled by improved processing methods (i.e., better solidification control). The latter types can be better controlled by composition modifications (i.e., lower carbon contents), and by improved melt and refractory practices. In characterizing the defects in directionally solidified (DS) superalloy castings, Narder and Kortovich (4) indicated that the dross (oxide) inclusions were found to be the single most frequent cause for casting rejections. Studies on P/M nickel-base superalloy materials have shown that the minimum low cycle fatigue life (LCF) is set by the presence of small, nonmetallic oxide inclusions in the material (5,6). Oxide inclusions having cross sectional areas as small as 8 $mils^2$ (0.005 mm^2), or less, have caused LCF failures in test specimens of P/M alloys (7).

The need for cleaner superalloys is approaching the limits of cleanliness by the conventional VIM processing route. Metal filtration using various types of ceramic filter media has been found to be an effective means of controlling the level and particle size of inclusions. It is interesting to note that melt refining via filtration has been an effective and well established commercial process in the aluminum industry (8) for over 15 years. The difficulty however has been to quantitatively assess the level of refinement. The electron-beam (EB) cleanliness evaluation test has been found to be a reproducible and a reliable method of assessing the level of melt cleanliness. Ceramic foam filters having a relatively high, open-pore volume have been utilized to produce clean melts of 713LC; 718; 738; and MM200 containing H_f.

Metal Filtration Technology and Principles

Removal of inclusions from the melt by the use of ceramic filters occurs not because of physical separation alone, but rather due to impingement and to the "manipulation" of the fluid flow within the porous medium. Essentially the process is a serial one in that the following two phenomena must take place:

- fluid flow conditions are manipulated such that the inclusions and the particulates to be removed are brought in contact with the filter walls, and subsequently
- capture at the filter wall occurs due to secondary forces as well as sintering of the inclusions.

Some newer developments in high-temperature ceramic filters have resulted in: 1) extruded, continuous, fixed-pore geometry ceramic monoliths and, 2) reticulated (foam), open-pore ceramic foams (9,10). The ceramic foams are currently available in a variety of refractory compositions and pore sizes, and genrally contain 75 to 90 percent of volume of open pores. In this paper the emphasis has been placed on the use of the ceramic foams because of their greater open porosity and because the pores are interconnected in such a manner that the melt must proceed through the filter by a tortuous path (which favors greater particle contact with the filter wall or web). Alumina ceramic foam filters (11) have recently been developed which resist crumbling due to handling, resist spalling due to thermal shock, and also resist creep deformation under the load of metal flowing at temperatures as high as 1700°C. An additional advantage of these new filters is that they do not have to be preheated prior to contact with the hot metal because of the high open porosity (75-90 vol.%) and because of the thinness of the cell walls.

Ceramic foams are classified in terms of the number of pores per linear inch (ppi) and a variation in the pore diameters throughout the foam exists. For a 10 ppi foam the average diameter is about 1778μm with a range of 584 - 3708μm; for a 30 ppi foam, the average diameter is 711μm, with a range of 229 - 1422μm.

The ability of a filter to capture (remove) particles from melt depends on many factors, such as: the connection and type of particles in the melt; the melt characteristics (composition, viscosity, surface tension); the temperature,; and the filter characteristics (composition, structure, porosity, permeability, etc.). A discussion of these factors is beyond the scope of this paper. However, for a given filter and cross sectional area, the flow rate of the metal passing through the filter and the thickness of the filter are two major factors affecting particle removal.

A relationship between the concentration of particles in a melt, the flow rate of the melt through a filter, and the reduced concentration of particles leaving a filter has been discussed in detail by Apelian and coworkers (9,10), which is shown as follows:

$$\eta = \frac{C_i - C_o}{C_i} = 1 - \exp\left[\frac{-K_o L}{U_m}\right]$$

where: η = the efficiency of particle removal
C_i = concentration of particles before filtration

C_o = concentration of particles after filtration

K_o = kinetic parameter coefficient

L = length of the filter

U_m = melt approach velocity.

On increasing the melt velocity, the filtration efficiency, η, will decrease from high to low values as shown by the curve in Figure 1. While experimental curves have been developed for aluminum, they have yet to be demonstrated for superalloys. Also, the relationship between the thickness of the filter necessary to produce a desired filtration efficiency for a given melt velocity needs to be established for high temperature alloys.

Two mechanisms predominate in the removal of particles when melts pass through ceramic filters, as shown in Figure 2. The first is a simple mechanical screening or blockage of coarse particles at the surface of the filter. The second involves the entrapment of smaller particles on the interior surfaces of the filter. The ability of a filter to entrap particles depends on the relative interfacial surface energies between the melt and the particles. If the interfacial energy is high (non-wetting), the particles will be "pushed out" of the melt when they contact another solid surface, such as that of other particles, crucible walls, or the surface of filter materials. Once the particles come in contact with a solid surface, they become attached and bond to that surface. The thermal energy of the melt is sufficient for the particles to "sinter" to the walls of the filter, or "sinter" to the other particles already bonded to the filter. Thus, even if the web structure is totally covered with attached particles, the filter will continue to be active, since the attached particles will continue to capture other particles in the melt when they come in contact.

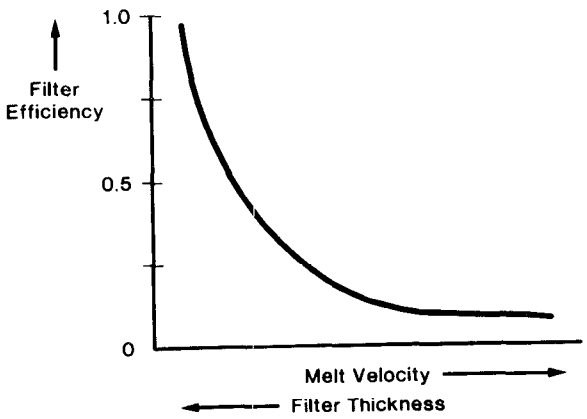

Figure 1: Effect of Melt Velocity and Filter Thickness on Filter Efficiency.

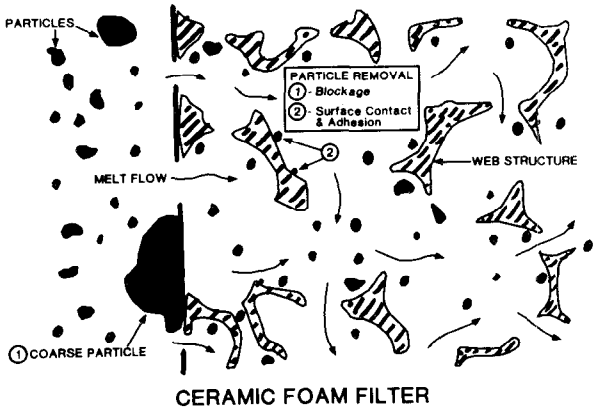

Figure 2: Particle Removal Mechanisms from Melt by 1) Blockage and, 2) Adhesion to Filter.

Filtration Experiments

Several Ni-base superalloys were melted using scrap material, most of which purposely contained hot tops, end crops and other pieces which were known to contain a relatively high non-metallic particle content. Over 50 13.5 kg (30-lb.) heats were melted and poured, with or without using filters, into ingot molds. Duplicate heats were made of each test condition, and the melting sequence was randomized with regards to filter material, alloy, and filtered and unfiltered heats, in order to minimize

the effects of any systematic variables. The cleanliness of the ingots was determined semiquantitatively from measurements of the area occupied by nonmetallic particles concentrated in electron beam melted specimens, which will be described later. Based on this cleanliness data, the effect of several variables (such as alloy composition and initial particle concentration, and filter composition) on the effectiveness of a given filter to remove particles from the melt could be assessed.

Materials

Alloys. Four nickel-base superalloys, which are typically used by the investment casting industry, were selected for this study, and their compositions are shown in Table I.

Table I - Composition of Alloys

Alloy	Ni	Co	Cr	Fe	Mo	W	Ta	Al	Ti	Nb	C	B	Zr	Hf
713LC	75	--	12.0	--	4.5	--	--	5.8	0.6	2.0	0.05	0.010	0.10	--
718	53	--	19.0	18.2	3.0	--	--	0.5	0.9	5.2	0.04	0.006	--	--
738	61	8.5	16.0	--	1.8	2.6	1.7	3.5	3.5	0.9	0.17	0.010	0.10	--
MM200 + Hf	60	9.5	8.5	--	--	12.0	--	5.0	2.0	1.0	0.10	--	--	1.8

Filter Materials. Ceramic foams, which were especially developed for high temperature applications(11),were used as the filter media. Such foams have a relatively high, open-pore volume, and can be fabricated in a variety of pore sizes. In this study, most of the filters contained about 20 pore per inch (ppi); the average pore diameter being about 1016μm (0.040 in.). Because of their open structure, the coarser foams (including 20 ppi) offer little resistance to metal flow, and at the same time force the melt to follow a tortuous path through the filter, which greatly enhances filtration efficiency. Four different filter compositions were used in the experiments (Table II).

Table II. Composition and Properties of Foam Filters (20 ppi)

Material	Composition (w/o)					* CTEx10^{-6}	Unit Bulk Density	Unit Porosity	Transverse Strength	
	Al_2O_3	SiO_2	MgO	ZrO_2	Y_2O_3	(cm/cm/°C)	(gm/cc)	(%)	(MPa)	(Psi)
NCL-Mullite	65	35	--	--	--	4.30	0.56	79	2.34	340
ZrO_2(stab.)	--	--	--	97	3	4.92	0.59	89	nd	nd
$ZrSiO_4$	--	33	--	67	--	4.40	0.58	81	0.34	50
Al_2O_3	92	7	1	--	--	7.89	0.58	80	2.62	380

*CTE = Coeff. of thermal expansion.

Experimental Filtration Procedure

The 13.6 kg heats were melted inductively in a vacuum furance under pressures of 0.4-1 microns (10^{-3} torr). The pouring temperature was standardized at 1510°C (2750°F) for all heats.

Prior to the pour, a 76 mm (3 in.) diameter ingot mold, which had been thoroughly cleaned and dried at 315°C (600°F) was placed in an isolated mold chamber located below the furnace. Ceramic pour cups, containing 25mm-thick filters, were peheated to 1090°C (2000°F) in a

nearby furnace, and immediately before a pour, the cup/filter unit would be transferred to the top of the mold in 6-8 sec. Pour cups, without filters for the control heats, were also heated and transferred in a similar manner. After the pour cup had been placed on top of the mold, the mold chamber would be immediately closed and pumped down to about 10 microns pressure before opening the valve to the furnace. The mold would then be raised hydraulically through the valve and into the furnace, so that the pour cup would be located about 300 mm (12 in.) below the crucible lip. The time from the transfer of the pour cup to the time of the pour would typically require 130 to 150 seconds. A sequence of the pouring events are shown in Figure 3.

After cooling, samples would be cut (Figure 3) from the ingot, and then would be remelted in an electron beam (EB) furnace for a cleanliness evaluation.

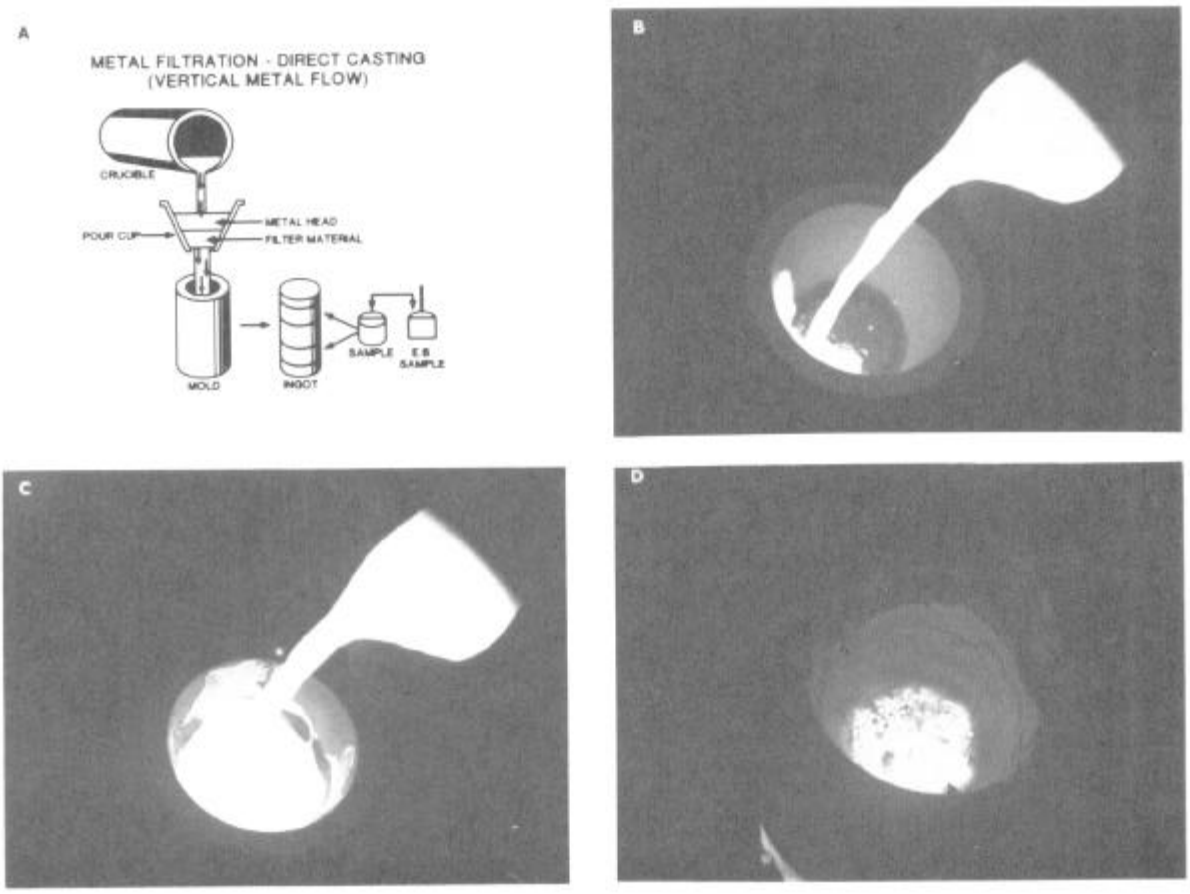

Figure 3: Procedure Used to Filter 13.6 Kg (30 lb.) Heats. Note Retention of Dross on Filter Surface (D). (Ref. 11)

Ingot Cleanliness Evaluation

The electron beam (EB) cleanliness test was used in this study because it provides a means to determine the non-metallic particle (inclusion) content within the volume of a sample. This test is proving to be especially effective for superalloys, where the inclusion levels are typically in the very low ppm (parts per million by weight) range(6,12-14).

The technique involves the drip-melting of a 1.4-2 kg (3-4 lb.) sample under a vacuum using an electron beam, and collecting the molten metal in a hemispherical, water-cooled copper mold. The procedure eliminates any further contamination from crucible materials. During the melting and solidification of the EB-specimen (button), the nonmetallic particles rise to the surface and are subsequently concentrated in a central floating raft. The particles in the raft can be removed chemically for a quantitative analysis, or can be observed directly using optical, SEM, image-analysis or other techniques. In this study, estimates of the nonmetallic particle content were made from area measurements of magnified photos of the rafts. The cleanliness was then determined by the size of the specific raft area (i.e., cm^2 per kg of sample); the smaller the specific area, the cleaner the sample. The details of the sample preparation, EB-melting, and evaluation are discussed in Reference 13.

The composition, shape and size of the particles were examined using SEM analysis. The EB-buttons, which weighed 0.68 kg (1.5 lb.) could be placed directly into the SEM, so that there was no need to remove or alter the raft of particles by further preparation. Figure 4A shows a typical EB-button, with a central raft of particles on the top surface. In this sample, the raft consisted of two regions; an outer zone of very fine Ti (C, N) particles surrounding a cluster of oxides (Figure 4B). This becomes evident from the Ti and Al x-ray maps of the same area (Figure 4C & D). Cross sections through this raft also indicated that not all of the very fine Ti(C,N) particles had floated (Figure 4E). However, the coarser oxide particles were effectively collected at the surface (Figure 4F).

Experimental Results

The data for the filtered and unfiltered heats are summarized in Table III and Figure 5, and are based on duplicate heats for each test condition. Two samples, one top and one bottom, were taken from each ingot; which represents about 10% of the ingot volume being anaylzed for the nonmetallic particle content.

The pour rates through the 20 ppi filters varied over a wide range (0.34 to 1.16 kg/sec.), which resulted largely from variations in the pore size between different compositions (due to different firing shrinkage) and in the plugging of pores by captured particles. In general, the pour rates through IN-718 and MM-200+Hf were slightly greater than for IN-713LC and IN-738. The variations in the pour rates for the 20 ppi filters did not appear to have an effect on filter efficiency. However, the slowing down of the pour rate to 0.11 kg/sec. for IN-738 by using a throttle or choke (with a 5 mm hole) below the filter significantly increased the filter efficiency from 83-84% to 96% (Table III). Also, the 30 ppi filter (with a smaller pore diameter of 711 μm or 0.028 in.) reduced the flow rate to 0.08 kg/sec. for the MM-200+Hf heat, and coupled with the finer pore size and greater surface area of the filter, the filtration efficiency was increased from 74-77% to 92% (Table III).

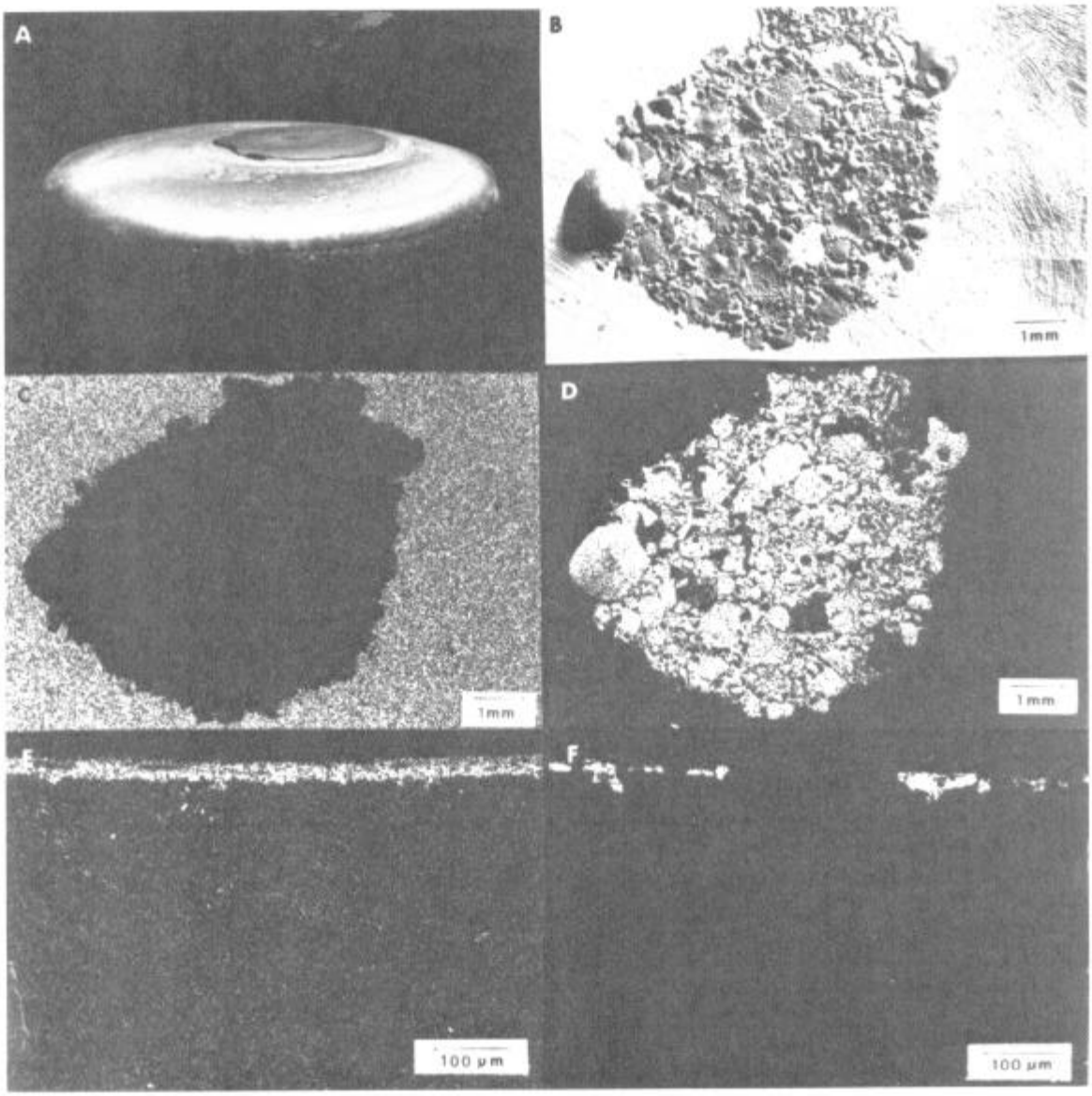

Figure 4: Photos of Particle Rafts on Top of IN-718 EB-Buttons. Photos B, C, D Show SEM Image, Ti and Al X-ray Maps, Respectively. Photos E & F Show Ti and Al Map of Cross Section Through Ti(C,N) and Al_2O_3 Rafts (Ref. 13).

Table III. Data on Filtered and Unfiltered Heats of Various Superalloys

Alloy	Filter Type	Pour Rate (kg/sec.)	Pour Rate (lb./sec.)	Specific Oxide Area (cm^2/kg)	Filter Efficiency (%)
IN-713LC	NCL-20 ppi	0.91	2.01	0.23	43
	Al_2O_3-20 ppi	0.85	1.87	0.18	55
	Control (No Filter)	0.79	1.76	0.40	--
IN-738	NCL-20 ppi	0.86	1.90	0.20	83
	$ZrSiO_4$	0.34	0.76	0.18	84
	NCL+Throttle	0.11	0.26	0.05	96
	Control	0.36	0.81	1.15	--
IN-718	NCL-20 ppi	1.11	2.44	0.03	97
	Control	0.84	1.84	1.05	--
	$ZrSiO_4$-20 ppi	1.16	2.55	0.03	96
	ZrO_2-20 ppi	0.87	1.91	0.04	94
	Control	0.74	1.62	0.74	--
	NCL-20 ppi Monolithic (264 cells/in^2)	1.00	2.20	0.07	76
	Control	1.28	2.81	0.11	62
		0.96	2.11	0.28	--
MM-200+Hf	$ZrSiO_4$-20 ppi	0.97	2.14	0.71	74
	NCL-20 ppi	1.16	2.55	0.62	77
	Control	0.29	0.65	2.69	--
	NCL-30 ppi	0.08	0.18	0.47	92
	NCL-20 ppi	0.60	1.32	1.43	75
	Control	0.42	0.92	5.70	--

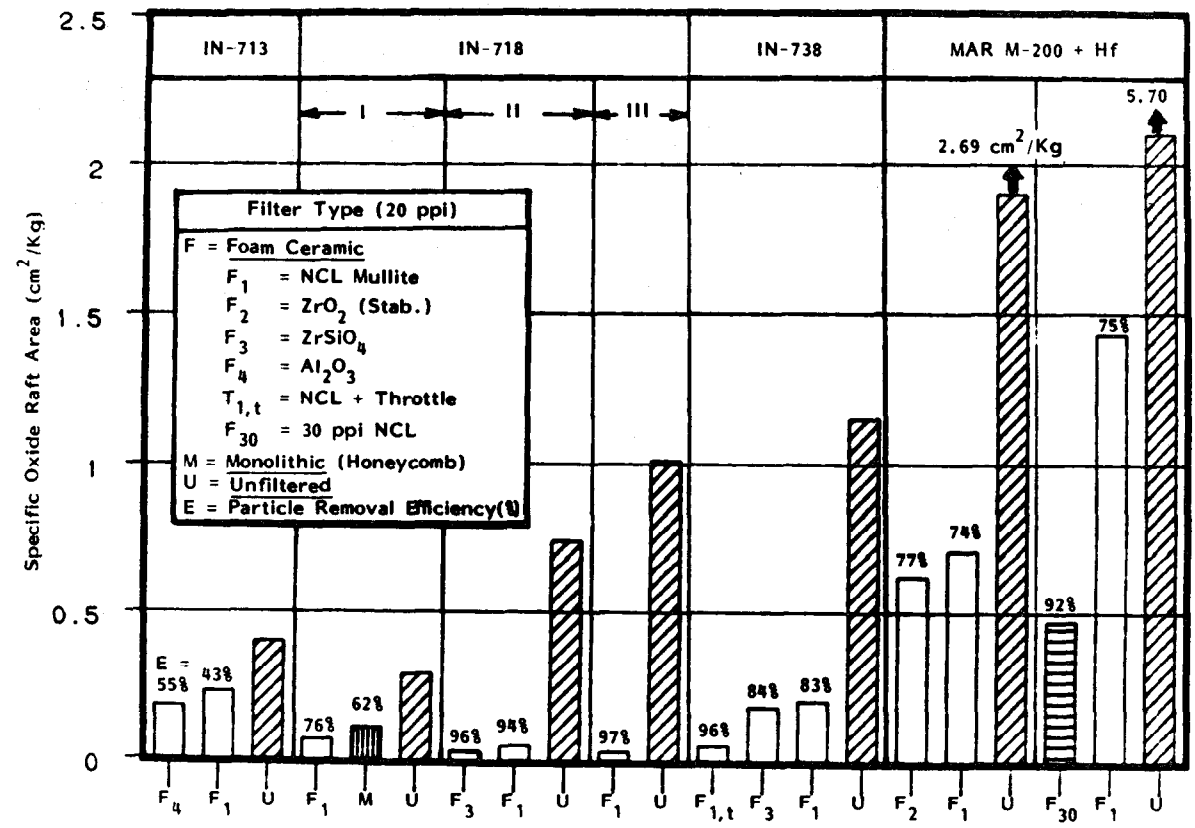

Figure 5: Effect of Different Filter Materials and Initial Heat Cleanliness on the Filtration Efficiency of Several Superalloy Melts.

Discussion

Figure 5 indicates that the application of ceramic filters to superalloy heats can significantly reduce the nonmetallic particle content of the melt. Further, the efficiency of the filter to remove particles from the melt is dependent on alloy composition, on initial particle concentration in the melt, on the pore size of the filter, and on the rate of flow through the melt (viz., at rates of 0.08 to 0.11 kg/sec vs. 0.3-1.3 kg/sec). The composition of the foam filter in most cases did not appear to affect filter efficiency in these studies.

With regards to initial particle concentration, the heats of IN-718 with specific oxide areas greater than 0.5 cm^2/kg (Fig. 5) were efficiently filtered, whereas those with a value less than 0.5 cm^2/kg (viz., 0.28 cm^2/kg) were not as efficiently filtered (E = 76% vs. E = 97%-96% for the dirtier heats). The monolithic filters did not appear to be as efficient as the foam filters in these tests (E = 62% vs. E = 76%). Alloys such as IN-713LC were not efficiently filtered by the foam filters, although the Al_2O_3 (E = 55%) composition was more efficient than the mullite (E = 43%). Also, the initial particle content of the starting scrap was low (viz., less than 0.5 cm^2/kg), which may also affect the overall filter efficiency. In the case of very dirty (high nonmetallic particle content) scrap with specific oxide content of above 2 kg/cm^2, the filter efficiency is relatively low (E = 77-77%) in the case of the MM-200 Hf; the lower efficiency may be also affected by the alloy composition, especially since HfO_2 particles are present in significant quantities. By using the finer 30 ppi pore size filter, which also reduces the metal flow rate through the filter, the efficiency of filtration for the Hf-bearing alloy was increased from 74-77% to 92%.

A SEM analysis of the oxides in the EB-button rafts from the various alloys showed that the particles were primarily oxides of aluminum, with minor and varying amounts of the Si, Mg, Ca oxides. On the other hand, HfO_2 was the primary oxide in the raft of the unfiltered MM-200+Hf, although its level was reduced significantly in the rafts from the filtered heats. Examination of the used filters showed that a significant concentration of the oxides and Ti-rich nitrides in the melt were deposited on the surfaces of the filters. Figure 6 shows a layer of these oxides and nitrides on a filter through which melt of IN-718 was poured.

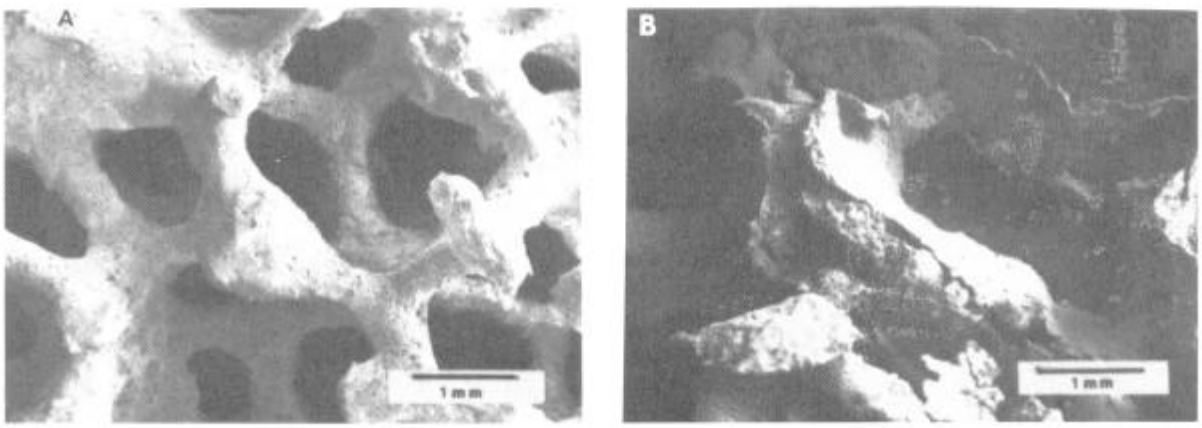

Figure 6: Front Surface of Filter Before (A) and After (B) Filtering IN-718. Note Attached Layer of Oxides and Nitrides Removed from the Melt.

The ability of a given filter to capture (remove) nonmetallic particles from the melt depends on relative surface energies of the filter materials, the nonmetallic particles, and on the surface tension (and composition) of the melt. Unfortunately, there are very little data on the surface tension of the superalloys and on the interfacial energies between the alloys and the oxides or nitrides of interest. Such information is necessary in order to predict filter efficiencies for a given filter/alloy system. Work is under way to determine these parameters both on the modeling and experimental fronts.

This study has shown that while the predominant oxides were Al_2O_3 (or rich in Al_2O_3), the ability of the filter to remove these oxides was dependent on the alloy composition. For example, the filter efficiency (for 20 ppi pore sizes) decreased in the following order: $E_{718} > E_{738} > E_{MM200+Hf} > E_{713LC}$. Only in the case of the MM200+Hf, the composition of the filtered EB-rafts was significantly different from that of the unfiltered rafts, where the former exhibited a high HfO_2/Al_2O_3 ratio (up to 40:1) and the latter a lower ratio (i.e., 10:1).

Also, the amount of Hf+Al oxides in the filtered EB-raft was lower, as shown in Figure 7, which also compares the rafts of unfiltered and filtered specimens of the alloys investigated. Figure 7B (filtered) shows a small raft of oxide particles lying on the surface of the alloy dendrites (MM-200+Hf). The unfiltered raft of particles (Figure 7A) is so large that the entire field at the same magnification is corrected with Al+Hf oxides.

The effect of filtration in IN-738 is clearly evident in Figure 7, where the (B) SEM photo shows only a few patches of oxides on a smooth, very thin nitride film. For IN-713, the filter efficiency was low (E = 43-55%), however, the size of the oxide particles was greatly reduced in the filtered heat (B-photo). X-ray maps of Al for 718 EB-raft specimens indicate a significant removal of the Al_2O_3-rich particles, in a filtered heat, and also, that the size of the remaining particles was much smaller.

Conclusions

1. Ceramic foam filters have been successfully utilized to remove oxide inclusions from superalloy melts. Inclusion removal efficiencies of up to 97% have been achieved.

2. For a 20 ppi pore size foam filter, the filter efficiency (E) decreased in the following order: $E_{718} > E_{738} > E_{MM200+Hf} > E_{713LC}$.

   The ability of the ceramic foam filter to remove and capture inclusions depends on the alloy composition and thus on the relative surface energies of the filter materials, the nonmetallic particles, and on the surface tension of the melt.

3. The electron beam cleanliness evaluation test has been found to be a reproducible and a reliable method of quantitatively assessing the level of melt cleanliness and filter performance.

Acknowledgements

The authors acknowledge J.S. Palmer for conducting the filtration studies and J.R. Morris for the data on the filter materials.

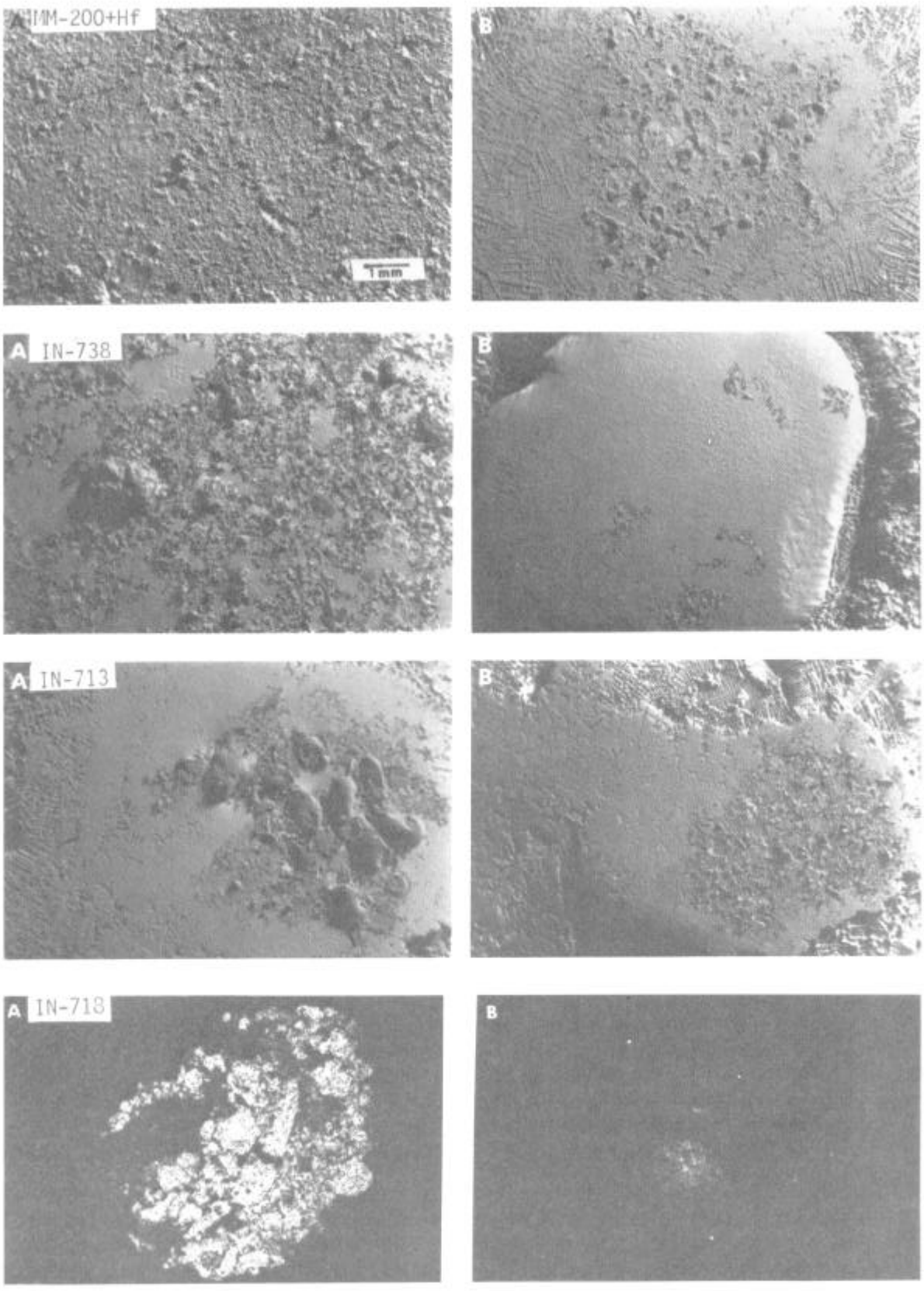

Figure 7: SEM Photo of Particle Rafts on EB-Buttons from Unfiltered (A) and Filtered (B) Heats. Photos of 718 are Al-X-ray Maps; Note Reduction of Al_2O_3 Particles in (B). (All Photos Same Mag.)

References

1. G.W. Meetham, "Superalloy Processing and Its Contributions to the Development of the Gas Turbine Engine", High Temperature Alloys for Gas Turbines , Applied Science Pub., London, pp. 837-859, 1978.

2. S.R. Houldsworth, "The Significance of Defects in Nickel-Base Superalloys", Superalloys '80, Proc. 4th Int. Symp. of Superalloys, ASM, pp. 375-383, 1980.

3. E. Bachelet, "Quality Castings of Superalloys", High Temperature Alloys for Gas Turbines, Applied Sci. Pub., London, pp. 665-699, 1978.

4. J.M. Narder and C.S. Kortovich, "Characterization of Casting Defects in Typical Castings of a Directionally Solidified Superalloy", Final Rept. AFML-TR-79-4060, TRW Materials Tech. Lab., Cleveland, OH, Contract F33615-76-5373, June, 1979 .

5. C.E. Shamblin, R.F. Halten, and W.R. Pfouts, "Manufacturing Methods for Improved Superalloy Powder Production", AFML F33615-78-e-5225, Second Interim Report.

6. E.E. Brown, J.E. Stulga, L. Jennings and R.W. Salkeld, "The Influence of VIM Crucible Composition, Vacuum Arc Remelting, and Electroslag Remelting on the Non-metallic Inclusion Content of Merl 76", Superalloys '80, Proc. 4th Int. Symp. on Superalloys, ASM, pp. 159-162, 1980.

7. J.D. Buzzanell and L.W. Lherbier, "Processing Effects on the Properties of P/M Rene 95 Near Net Shapes", Superalloys '80, Proc. 4th Int. Symp. on Superalloys, ASM, pp 149-158, 1980.

8. L.C. Blayden and K.J. Brondyke, "In-Line Treatment of Molten Aluminum", Light Metals, AIME, pp. 473-503, 1973.

9. D. Apelian and R. Mutharasan, "Filtration: A Melt Refining Method", J. Metals, 32 (9), pp. 14-19, 1980.

10. R. Mutharasan, D. Apelian and C. Romanowski, "A Laboratory Investigation of Aluminum Filtration Through Deep-Bed and Ceramic Open-Pore Filters", J. Metals 33 (12), p. 12-17, 1981.

11. W.H. Sutton and J.R. Morris, "Development of Ceramic Foam Materials for the Filtration of High-Temperature Investment Casting Alloys", 31st Ann. Mtg., Investment Casting Inst., Dallas, TX, Oct. 5-7, 1983.

12. W.H. Sutton, G.E. Maurer, J.A. Domingue and I.D. Clark, "Determination of Nonmetallic Particle Content and Composition to Improve Primary Melt Cleanliness of Superalloys", 29th Ann. Mtg., Inves. Casting Inst., Scottsdale, AZ, Oct. 15-17, 1981.

13. W.H. Sutton and I.D. Clark, "Development of an EB Melting Test to Evaluate the Cleanliness of Superalloys", Electron Beam Melting and Refining, State of the Art, 1983, Bakish Material Corp., Reno, NV, Nov. 1983.

14. C.E. Shamblen, S.L. Culp and R.W. Lober, "Superalloy Cleanliness Evaluation Using the EB Button Melt Test", Electron Beam Melting and Refining, State of the Art, 1983; Bakish Materials Corp., Reno, NV, Nov. 1983.